their use for the synthesis of metallic and organic nanostructures. *Nucl. Instrum. Methods B*, 2002, **196**, 81.
6. Molares, M. E. T., Hohberger, E. M., Schaeflein, C., Blick, R. H., Neumann, R. and Trautmann, C., Electrical characterization of electrochemically grown single copper nanowires. *Appl. Phys. Lett.*, 2003, **82**, 2139.
7. Schuchert, I. U., Molares, M. E. T., Dobrev, D., Vetter, J., Neumann, R. and Martin, M., Electrochemical copper deposition in etched ion track membranes – Experimental results and a qualitative kinetic-model. *J. Electrochem. Soc.*, 2003, **150**, C189.
8. Tian, M. L., Wang, J. U., Kurtz, J., Mallouk, T. E. and Chan, M. H. W., Electrochemical growth of single-crystal metal nanowires via a 2-dimensional nucleation and growth-mechanism. *NanoLetters*, 2003, **3**, 919.
9. Cai, Z. and Martin, C. R., Electronically conductive polymer fibrils with mesoscopic diameters show enhanced electronic conductivity. *J. Am. Chem. Soc.*, 1989, **111**, 4138–4139.
10. Chakravarti, S. K. and Vetter, J., Morphology of etched pores and microstructures fabricated from nuclear track filters. *Nucl. Instrum. Methods B.*, 1991, **62**, 109–115.
11. Dai, H., Hafner, J. H., Rinzler, A. G., Colbert, D. T. and Smalley, R. E., Nanotubes as nanoprobes in scanning probe microscopy. *Nature*, 1996, **384**, 147–150.
12. Dobrev, D., Vetter, J. and Angert, N., An electrochemical cell for microgalvanic filling of etched tracks in organic polymers. GSI Sci. Rep., Darmstadt, Germany.
13. Fischer, B. E. and Spohr, R., Production and use of nuclear tracks: Imprinting structures on solids. *Rev. Mod. Phys.*, 1983, **55**, 907–948.
14. Foss, C. A., Hornyak, G. L., Stockert, J. A. and Martin, C. R., Template synthesized nanoscopic gold particles: Optical spectra and the effects of particle size and shape. *J. Phys. Chem.*, 1994, **96**, 2963–2971.
15. Frazier, A. B. and Allen, M. G., Metallic microstructures fabricated using photosensitive polyimide electroplating molds. *J. Microelectromec. Syst.*, 1993, **2**, 87–93.
16. Granstrom, M., Berggren, M. and Inganas, Micrometer and nanometer sized polymeric light emitting diodes. *Science*, 1995, **267**, 1479–1481.
17. Klein, J. D., Herrick, R. D., Palmer, D., Sailor, M. J., Brumlik, C. J. and Martin, C. R., Electrochemical fabrication of cadmium chalcogenide microdiode arrays. *Chem. Mater.*, 1993, **5**, 902–904.
18. Martin, C. R., Nanomaterials: A membrane based synthetic approach. *Science*, 1994, **266**, 1961–1966.

ACKNOWLEDGEMENTS. S. K. thanks Council of Scientific and Industrial Research, New Delhi for providing financial assistance in the form of Senior Research Fellowship.

Received 6 March 2004; revised accepted 19 July 2004

Electronic biopsy for skin cancer detection

G. Florence Sudha* and T. Ganesa Palnivelu
Department of Electronics and Communication Engineering, Pondicherry Engineering College, Pondicherry 605 014, India

Assessing tissues without their removal is a great advantage. A tissue biopsy removes tissue, which yields a wound that requires healing. Healing may cause discomfort to the patient and may yield a scar. This communication proposes an optoelectronic biopsy, employing light source and optical fibres. This reflectance imaging system permits imaging of the tissue so as to discriminate the cancerous ones without removal of tissues for analysis. This system based on the principle of backscattering of laser radiation from tissue promises to be a low cost, accurate and fast tool for detection of skin cancer.

SKIN cancer is the most frequently occurring of all cancers. Each year over 500,000 new cases of skin cancer are detected. In a high percentage of skin cancers fatalities can be all but eliminated and morbidity reduced, if detected early and treated properly. These skin lesions are distinguished generally by subjective visual inspection and their definitive diagnosis requires time-consuming, expensive histopathological evaluation of excisional or incisional biopsies.

There are three main types of skin cancer–malignant melanoma, basal cell carcinoma and squamous cell carcinoma. Melanoma is less common, but the most serious type. It can spread if not detected at an early stage. It often spreads to other tissues or vital organs. Melanomas are irregular in shape, show variation in colour and are lesions bigger than 6 mm across. Basal cell carcinoma is the most common type of skin cancer. It grows slowly and can damage nearby tissues. It arises from cells in the epidermis. It is not life-threatening, but if left untreated, cancerous cells can grow deeper into the skin. Squamous cell carcinoma is the most common type of skin cancer. It arises from cells in the epidermis and can spread to nearby lymph nodes. It can be dangerous because it grows more quickly.

Other skin infections are Actinic keratosis and Bowen's disease that can become malignant. The condition is harmless, but if left untreated it may transform to squamous cell carcinoma. Seborrheic keratosis is a benign form of skin tumour occurring in the outer layers of the skin. Compound nevus is characterized by proliferation of nevus cells within the basal cell layer of the surface epithelium and the underlying connective tissue.

Currently, the majority of skin cancers are confirmed using an invasive biopsy. This means that a section of the

*For correspondence. (e-mail: gfsudha@eth.net)

skin must be removed and then studied in the laboratory. Results can take anywhere from three to ten days. Merely 20% of the biopsies performed, however, diagnose a malignancy. People anxious about being poked or cut, delay or avoid seeing a doctor. Also, there are recorded histories of patients who do not show primary symptoms on the surface of the skin, but the disease had already entered into the lymph nodes. Some skin cancers are slow-growing, but can metastasize quickly to other parts of the body through the blood or the lymph nodes.

All these have compelled for a non-invasive approach, where the patient will have a fast and accurate method of detection, undergo less pain, less bleeding and have greater comfort in the quality of care provided by the doctor.

This research proposes to build an optical-fibre reflectance imaging system using a light source and an optical fibre bundle. This device will be able to measure tissue optical properties and detect skin cancers *in vivo*, non-invasively and quickly. *In vivo* experimental evidence has shown that cancerous skin lesions have different optical properties compared with non-cancerous lesions or normal skin. Therefore, cancerous ones may be differentiated from non-cancerous skin lesions by comparing the optical properties of the skin lesions with those of the surrounding normal skin sites.

Another potential application could be in the study of skeletal blood flow. Optical techniques provide a non-invasive solution to assess changes in skin blood circulation and oxygen saturation. The intensity of the reflected and scattered light recorded is assumed to be related to blood perfusion changes underneath the probe. Using the designed imaging system, a non-invasive and continuous assessment of local muscle blood flow is possible.

The skin structure is composed of two primary layers – the epidermis and the underlying dermis. The epidermis consists of keratinizing sublayers supported by the dermal layer of dense fibro elastic connective tissues containing glands and hairs. The average thickness of the epidermis is approximately 3 mm and that of the dermis is between 50 and 150 μm. The dominant absorber of laser radiation in the epidermis is melanin and in the dermal layer, the principal absorber is haemoglobin. In the epidermis, absorption of melanin rapidly increases as wavelength decreases. The penetration of laser light at the therapeutic window (600–1300 nm) owes more to scattering and absorption. This allows for substantial penetration of light in the tissue and high remittance of the light scattered out of the tissue after deep penetration.

Accurate understanding of the optical properties of the human skin remains a challenge to biomedical optics, and theoretical modelling of light propagation in skin tissue continues to be active. The effect of skin tissue structure on light distribution has been investigated through various layer models[1–4]. It is well known that the skin interfaces

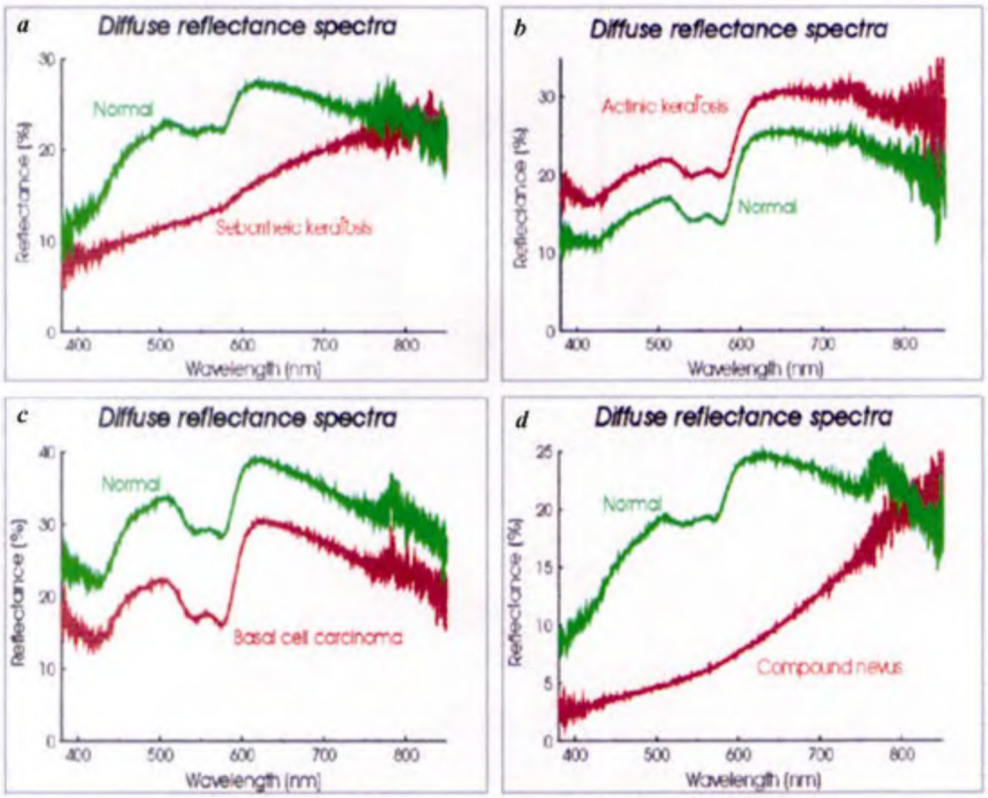

Figure 1. Diffuse reflectance spectra for various types of skin malignancies.

are inherently rough, and interface roughness has been taken into account in the model for qualitative understanding of its effect on light distribution[5]. Pioneering work on the possibility of reflectance imaging using the integrating sphere was done by Singh[6]. Recently, by the measurement of diffusely backscattered radiation, the internal structure of the human forearm has been analysed[7]. Phantoms using white paraffin wax mixed with wax-coloured pigments proved to be equivalent to tissue[8]. The photon backscattering simulated images of a combination of tissues are obtained using the multiprobe laser reflectometer[9].

The reflectance spectra of different types of skin cancer have been studied[10]. Figure 1 *a–d* shows the comparison of diffuse reflectance spectra of seborrheic keratosis, actinic keratosis, basal cell carcinoma and compound nevus with normal skin.

The figure indicates that the reflectance spectra for cancerous cells are significantly different compared with normal skin. A lower value of reflectance indicates higher absorption of light by cancerous cells and a higher value indicates more scattering. This concludes that reflectance can be taken as a parameter for distinguishing between normal and malignant tissue. Hence measurement of the backscattered radiation using laser – fibre optic probe assembly provides images that can help fast detection and localization of skin cancer.

The objective of the work is to develop a device to measure backscattered radiation from the skin for the detection and localization of skin cancer. The schematic of the proposed device is shown in Figure 2. The source selected was a He Ne laser operating a 632.8 nm (Uniphase Inc, 1101P) and having a output power of 4 mW. Selection of the source was done based on the fact that the diagnostic technique requires the laser output power to be sufficient for optimum depth of penetration, such that the reflectance values can be measured but without causing tissue damage. The penetration depth of the He Ne laser is approximately 3 mm which is sufficient to map the epidermis and dermis. To minimize the losses, an additional focusing lens of magnification 20X was used. This concentrates the incident light directly onto the fibre. A cylindrical probe made of stainless steel with diameter 2.5 cm and length 2 cm, has two sleeves made so as to accommodate two plastic fibres – an input fibre of length 50 cm and active diameter 0.1 cm, and an output fibre of length 25 cm and active diameter 0.1 cm. The input fibre is used to guide the laser light to the tissue and the output fibre is used for collecting the backscattered light to the photo detector. The centre-to-centre separation between the input and the output fibre was 0.4 cm. The probe is held in a PVC tube of length 2.1 cm, so that the probe is above the skin by 0.1 cm and the active region is not in contact with the skin. A low-noise, high-speed photodiode BPW34 is used to detect the backscattered low optical power.

The photo detection assembly shown in Figure 2, is well insulated from stray light and the fibre is guided and fixed in position using a plastic case with inlet for the fibre. A black casing ensures isolation of the coupling interface from the ambient light. The photocurrents are in the order of nA and are converted into voltages using TL084. The voltage levels obtained after conversion are in the mV range. Voltages of this order cannot be directly interfaced to the computer for further processing and hence need to be amplified. Amplification is done using IC 741 in the inverting mode. The complete signal conditioning circuit is shown in Figure 3. The output of this circuit is digitized using a 12 bit ADC card (OTS101 ADDA). This card has a conversion time of 25 µs and full scale output of 5V DC. This is interfaced to a Pentium processor for data acquisition and processing.

To demonstrate the potentiality of the reflectance imaging system in imaging malignancy below the skin, for detection of skin cancer, a tissue phantom made from gelatin was prepared in a petri dish. Gelatin was chosen for preparation of the phantom because its optical absorption coefficient can be easily changed in a wide range by varying the dye colour and concentration. The absorption spectrum of gelatin is different for different colours. Figure 4 shows the absorption spectrum of eight gelatin colours.

A jelly made of gelatin of thickness 5 mm for the base and another jelly layer of thickness 3 mm for the top layer were prepared. A jelly mixed with red food colouring substance of thickness 3 mm was also prepared. In the base jelly layer, a hole of diameter 1 cm was made by scraping out the jelly and a piece of the coloured jelly was inserted into the hole. Now the top jelly layer was placed to complete the malignant skin tissue phantom.

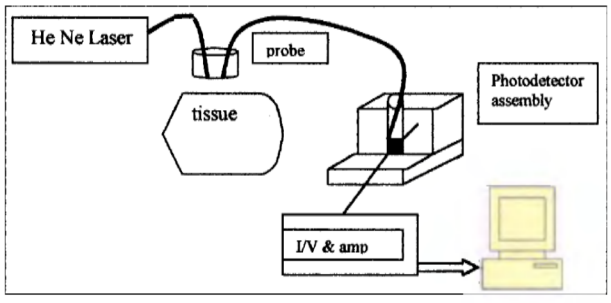

Figure 2. Schematic of the fibre optic reflectance imaging system.

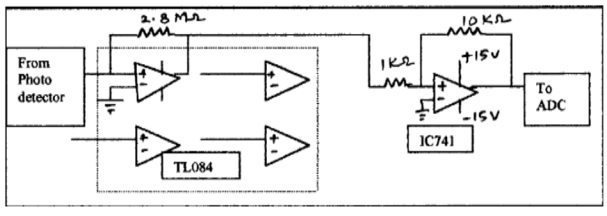

Figure 3. Signal conditioning circuit.

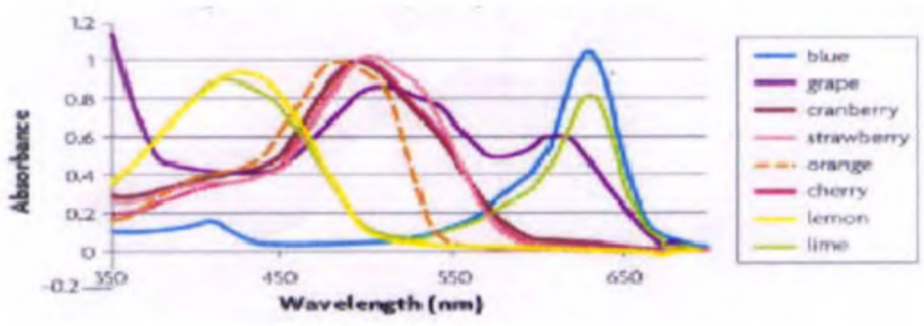

Figure 4. Absorption spectrum of different colours of gelatin.

For measurement of backscattered radiation, a 200 × 200 grid and the outline of the tissue phantom were developed. Observation points wherein data have to be obtained, were selected. The probe is placed over each of the location points for one second so that the output value at a particular point can be stored into the computer. The reflectance at each point represents an average of hundred samples, which was done so that the system, when used in a human subject, averages out the effects of pulsation due to blood flow. The probe is always held perpendicular to the surface of the tissue for maximum reflectance. Measurements are carried out at every 5 mm increment, horizontally, till the entire row is scanned and the process is repeated row by row. In this way, the entire phantom is scanned and the scan data values are stored.

The scan process being done manually, gives irregular points in the grid. To obtain all the points in the grid, interpolation using Pythagorean equation is carried out. Prior to testing on the phantom, the designed system is calibrated by placing the detector on black rubber for minimum reference value and white rubber for maximum reference value.

Software has been developed to obtain the reflectance images of the tissue.

An outline of the tissue to be imaged is drawn and divided into the same number of blocks as was done when measurements were taken manually, so the specific pixels have values corresponding to specific reflectance values. Using the maximum and minimum values obtained, the range of reflectance values is found and a colour code is devised. Each value from the data file is read and the colour corresponding to the value is assigned to a particular block. The process is continued in a fixed pattern for the 200 × 200 values, so that the entire outline is fixed with the specific colour code corresponding to the data locations. The image is passed through a two-dimensional averaging filter of size [5, 5] for the purpose of continuity. The final image is obtained after passing through a median filter, where each output pixel contains the median value in the 8 × 8 neighbourhood around the corresponding pixel in the input image.

Table 1. Losses encountered at various stages

Stage	Power	Loss (in dB)
After source	1.75 mW	3.59
After focusing lens	730 μW	3.8
At the end of input fibre	50 μW	11.687

The final incident power on the tissue in the order of 50 μW, is sufficient to image the tissue without resulting in damage of the erythrocytes in the region concerned.

Prior to incidence on the tissue, the laser light undergoes losses at various stages of coupling (Table 1).

Figure 5 *a* and *b* shows the images obtained using the laser reflectance imaging system. Figure 5 *a* is the image obtained without placing the coloured jelly and Figure 5 *b* is the image obtained after placement of the coloured jelly at a depth of 3 mm from the surface, to simulate the presence of cancerous tissue. From the images, the object placed at a depth of 3 mm from the surface layer is shown to be detected and the intensity is lower at the background than that for the object. The background is uniform, except for some scattering near the object.

The imaging system was used to image the forearm of human subjects to check its utility in human organs. Different subjects within the age group of 20–60 years were chosen on the basis of complexion and forearm images were obtained. A grid of size 200 × 200, wherein data have to be obtained, was first developed. The probe was placed over each of the location points for one second so that the output value at a particular point can be stored into the computer. Measurements were carried out at every 5 mm increment horizontally, till the entire row was scanned, and the process was repeated row by row. In this way the entire forearm was scanned and the scan data values stored in a computer. All intermediate values in the grid were calculated by interpolation using Pythagorean equation. The final images were obtained using the imaging algorithm.

The images of a brown- and dark-complexioned subject are shown in Figure 6 *a* and *b*. Images show a variation in reflectance, because it is affected by skin pigmentation. For the dark-complexioned subjects, higher absorp-

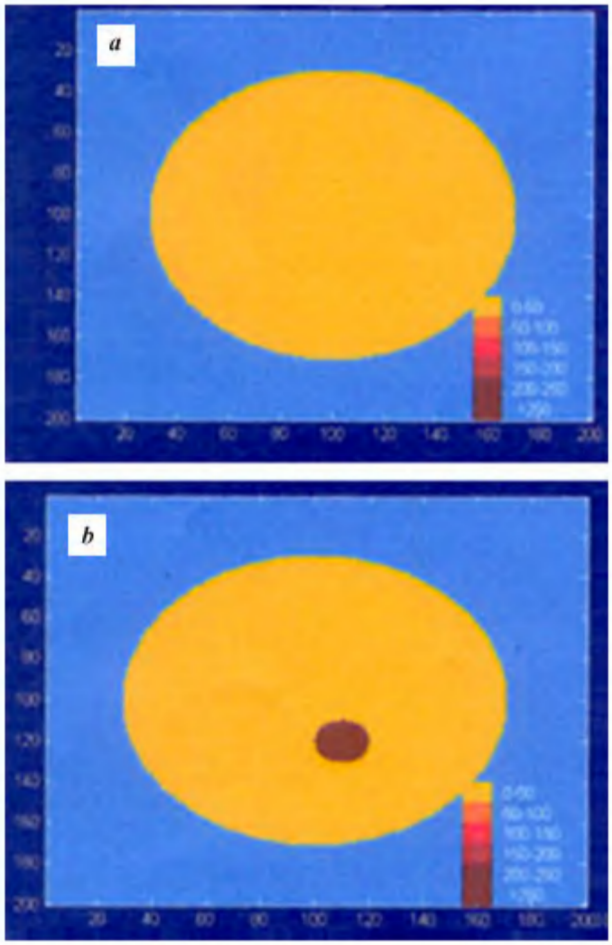

Figure 5. Image of a gelatin phantom without introduction of abnormality (***a***) and having abnormality (***b***).

tion in melanin causes reduction in reflectance values. The overall pattern obtained for the subjects is however similar.

Measurement repeatability was assessed by repeatedly imaging the left forearm of a brown-tone subject and the average error was found to be 0.12%.

A fibre-optic reflectance imaging system sensitive to the variation in tissue composition and blood flow underneath the skin, has been constructed and tested. The proposed device, which improves the abilities of the physician, can facilitate early screening and detection of skin cancers to maximize cure and reduce or even avoid unnecessary biopsies. Like a dental X-ray, an assistant is sufficient to do a scan on a patient, which it would take only a few minutes. Furthermore, these devices are portable and relatively inexpensive. Therefore, they can be used in remote rural areas and the diagnostic results can be easily transferred to metropolitan diagnostic centres via modems or the information superhighway in the near future for expert prognosis, if needed.

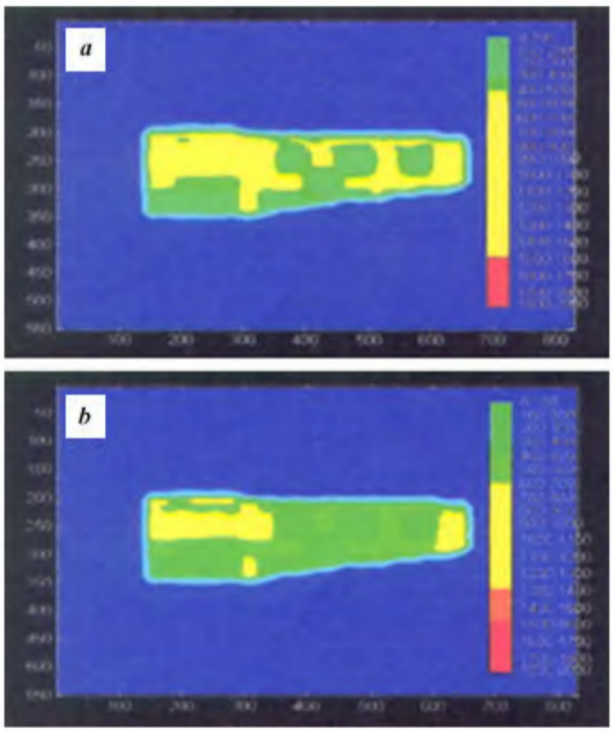

Figure 6. Comparison of reflectance images for different complexion subjects. Reflectance image of left forearm of brown-complexioned subject (***a***) and dark-complexioned subject (***b***).

1. Nossal, R., Keifer, J., Weiss, G. H., Bonner, R., Taitelbaum, H. and Havlin, S., Photon migration in layered media. *Appl. Opt.*, 1988, **27**, 3301–3382.
2. Schmitt, J. M., Zhou, G. X. and Walker, E. C., Multilayer model of photon diffusion in skin. *J. Opt. Soc. Am.*, 1990, **A7**, 2141–2153.
3. Cui, W. and Ostrander, L. E., The relationship of surface measurements to optical properties of layered biological media. *IEEE Trans. Biomed. Eng.*, 1992, **39**, 194–201.
4. Miller, I. D. and Veith, A. R., Optical modelling of light distribution in skin tissue following laser irradiation. *Laser Surg. Med.*, 1993, **13**, 565–571.
5. Jun Q. Lu, Xin-Hua Hu and Ke Dong, Modeling of the rough interface effect on a converging light beam propagating in a skin tissue phantom. *Appl. Opt.*, 2000, **39**, 5890–5896.
6. Singh, M., Helium neon laser screening of human body. *Med. Biol. Eng. Comput.*, 1981, **19**, 175–178.
7. Chacko, S. and Singh, M., Multi-layer imaging of human organs by laser backscattered radiation. *Med. Biol. Eng. Comput.*, 1999, **37**, 278–284.
8. Srinivasan, R. and Singh, M., Laser backscattering and transillumination imaging of human tissue and their equivalent phantoms. *IEEE Trans. Biomed. Eng.*, 2003, **50**, 724–730.
9. Kumar, D. and Singh, M., Characterization and imaging of compostional variation in tissues. *IEEE Trans. Biomed. Eng.*, 2003, **50**, 1012–1019.
10. Zeng, H., Lui, H., Macaulay, C., McLean, D. I. and Palcic, B., Optical spectroscopy studies of diseased skin – preliminary results. *SPIE J.*, 1995, **2628**, 281–285.

Received 24 February 2004; revised accepted 7 May 2004